Experimental and in-silico investigation of population heterogeneity in continuous Sachharomyces cerevisiae scale-down fermentation in a novel two-compartment setup.

Heins, Anna-Lena; Lencastre Fernandes, Rita; Gernaey, Krist; Eliasson Lantz, Anna

Published in:
Journal of Chemical Technology and Biotechnology

Link to article, DOI:
10.1002/jctb.4532

Publication date:
2015

Document Version
Peer reviewed version

Experimental and *in-silico* investigation of population heterogeneity in continuous *Sachharomyces cerevisiae* scale-down fermentation in a novel two-compartment setup

Anna-Lena Heins[1,2*], Rita Lencastre Fernandes[2*], Krist V. Gernaey[2] and Anna Eliasson Lantz[1, 2§]

[1] Department of Systems Biology, Technical University of Denmark, 2800 Kongens Lyngby, Denmark

[2] Department of Chemical and Biochemical Engineering, Technical University of Denmark, 2800 Kongens Lyngby, Denmark

*These authors contributed equally to the work

[§]Corresponding author, email: aela@kt.dtu.dk , phone: +4545252851

Abstract

Background. In large-scale bioreactors, microbes often encounter fluctuating conditions of nutrient and oxygen supply, resulting in different microbial behavior at the different scales. The underlying reason being spatial heterogeneity, caused by limited mixing capabilities at production scale. Consequently, scale-up of processes is challenging and there is a need for laboratory-scale reactor setups that can mimic large-scale conditions to enhance the understanding of how fluctuating environmental conditions affect microbial physiology.

This article has been accepted for publication and undergone full peer review but has not been through the copyediting, typesetting, pagination and proofreading process, which may lead to differences between this version and the Version of Record. Please cite this article as doi: 10.1002/jctb.04532

Results. A two-compartment, scale-down setup, consisting of two interconnected stirred tank reactors was used in combination with mathematical modeling, to mimic large-scale continuous cultivations. One reactor represents the feeding zone with high glucose concentration and low oxygen, whereas the other one represents the remaining reactor volume. An earlier developed population balance model coupled to an unstructured model[1] was used to describe the development of bulk concentrations and cell size distributions at varying dilution rate, glucose feed concentration as well as recirculation times between the two compartments. The concentration profiles of biomass and glucose could be successfully validated experimentally. Single cell properties of two fluorescent reporter strains, that were applied for deeper investigation of cell robustness characteristics and ethanol growth distributions, could be quantified compartment-wise revealing differences in cell population distributions related to environmental conditions and also compared to the one-compartment, conventional chemostat.

Conclusion. Results underline the utility for the here presented combined approach as well as the use of continuous scale-down reactors for process investigations as insights concerning single-cell characteristics of the process are revealed, which are normally hidden.

Keywords: population balance model, population heterogeneity, reporter strain, two-compartment bioreactor, mathematical modeling, continuous scale-down reactor

Introduction

Nowadays, theadvances in modeling allow the model-based description of single cell physiology in biotechnologicalindustrial fermentation processes[2]. Therefore, a systematic approach using modeling in combination with laboratory-scale experiments can be used to facilitate process optimization[3]. Whereas modeling can assist in setting the range of interesting experiments, evaluating experimental data, finding the performance optimum and

creating a framework for future process development, . In turn experiments are then used to collect data in setups simulating large-scale process conditions, to validate modeling results and iteratively improve the model. It is important to point out that Indeed the model validation step is indeed one of the most important parts of a modeling study.

Large-scale fed-batch and continuous cultivations are widely used in the biotechnology industry for the industrial production of pharmaceuticals, biomass and proteins (e.g. insulin)[4,5]. At large scale, gradients of process parameters (e.g. substrate concentration, pH and oxygen) arising due to non-ideal mixing behavior were found to be a major cause of cell population heterogeneity[6,7]. Especially substrate gradients contribute to this phenomenon because cells traveling throughout the reactor experience high substrate concentrations close to the feed port and low concentrations in zones more distant to the feed port. For *Escherichia coli*[6,7] this was found to be connected with elevated stress response, especially when cells pass the feeding zone. The use of Rushton turbines has also been observed to generate compartments within the reactor due to high axial flow barriers created by the turbine[8]. Gradients can result in lowered yields and a rise in by-product formation[9,10]. The understanding of population heterogeneity – population properties are rather distributed than following average characteristics[11] as earlier assumed – is important to understand process performance at larger scale, since cell population heterogeneity effects will complicate process optimization.

A crude and simple way of assessing the degree of spatial population heterogeneity in a bioreactor is the compartment model approach. In such an approach, it is assumed that the bioreactor is divided into different zones due to the non-ideal mixing patterns. Exchange flows connect the compartments (zones), and the higher the exchange flow between compartments, the closer to the ideal mixing case one is, i.e. a one compartment setup. In the

other extreme, the system can be represented using Computational Fluid Dynamics (CFD) simulations, where a large number of very small volume elements are considered. In a compartment model approach, an ideal mixing behavior, and thus a continuous stirred tank reactor (CSTR) description, can be assumed for each compartment (i.e. spatial zone). Besides offering a straightforward way for describing non-ideal mixing in large-scale reactors, a compartment model approach has the advantage of being easily translated into laboratory-scale experimental setups by using scale-down reactors.

Scale-down reactors are nowadays increasingly used for process development and optimization, and have been shown to be a valuable tool for the study of gradients of substrate, oxygen[12] and pH seen in large-scale fermentation processes[13]. Most commonly the scale-down reactor consists of stirred tank reactors (STR) connected to plug flow reactors (PFR) or two STRs connected to each other[14] because both setups allow the creation of gradients of various reactor parameters in a well-controlled environment, which is especially useful for studying population heterogeneity. Several studies investigated glucose gradients and the consequent averaged population properties e.g. during aerobic ethanol production[15], which revealed the induction of stress responses close to the perturbation zone as well as by-product formation in both *S. cerevisiae* and *E. coli*[16] (PFR connected to STR). Sweere *et al.* (1988)[17] investigated the effects of fluctuating glucose concentration on *S. cerevisiae* physiology, applying different circulation times and volume ratio of the two stirred tank reactors, while the feed was only added to the reactor with the smaller volume which revealed induction of stress responses as well as. Similar as for George *et al.* (1993)[15] in a setup with an STR connected to a PFR, induction of stress responses was found. Later Delvigne *et al.* (2006a, 2006b & 2006c)[18-20] developed, for both *E. coli* and *S. cerevisiae*, a combination of stochastic microbial growth and bioreactor mixing models to explore the hydrodynamic

effect of the bioreactor on microbial growth, which allowed explanation of the metabolic changes cells experience associated with glucose fluctuations. CBy combining the two model parts the authors could describe the concentration profiles that a cell was subjected to during its cultivation in the bioreactor. All above mentioned used setups have been performed in fed-batch mode, with one reactor representing the feeding zone and the other one the perturbation zone (either PFR with perturbation at inlet or STR with different conditions compared to the other one).

In this study, substrate gradients are simulated and the effect of the operating conditions (dilution rate and glucose feed concentration) is evaluated using, to our knowledge, for the first time a scale-down reactor system that operates in continuous mode including a waste outlet. The existence of gradients is assumed to result in a compartmentalization of the reactor (i.e. delimited spatial zones can be defined). This compartmentalization is translated into an experimental setup consisting of two compartments of different volume, one representing the feeding zone and one representing the remaining reactor volume where the bioreactor outlet, which has not been included into earlier setups published (see for overview[21]), is located. This study addresses firstly an *in silico* investigation of the dynamics of a yeast population cell size distribution during a continuous large-scale fermentation, where a compartmentalization of the reactor can be assumed. The performed computer simulations rely on an adaption of a previously described population balance model (PBM) coupled to an unstructured model describing the bulk concentrations in the cultivation media[1].

Following the *in silico* study, the corresponding experimental investigation was performed by running glucose-limited chemostat cultivations using growth and ethanol metabolism *S. cerevisiae* reporter strains. Yeast single cell physiology and robustness was assessed by flow

cytometry analysis. Apart from exhibiting general growth physiology the two strains used in this study express a fluorescent protein whose activity can be easily assayed[22]. In the major part of the cultivations performed in this studyMainly, the growth reporter strain FE440 was used: it expresses a green fluorescent protein (GFP) from a ribosomal promoter which enables monitoring of metabolic activity at single cell level[23]. It also allows for investigation of membrane robustness, when applying freeze-thaw stress to cells sampled from the fermentation broth membrane robustness could be investigated[23]. In some cultivations, an ethanol reporter Sc-PCK1-B expressing a blue fluorescent protein (TagBFP) from a phosphoenolpyruvate carboxykinase promoter (inactive when glucose is present, part of gluconeogenesis) whose expression is correlated to ethanol consumption (Johansen et al., unpublished) was utilized. Consequently, the use of flow cytometry analysis revealed not only distributions of cell size and morphology, but also metabolic activity and ethanol consumption characteristics of thousands of single cells per second. Thus, in addition to conventional growth physiology also differences in the expression profiles of reporter genes for single cells traveling throughout the scale-down system were investigated.

Materials and Methods

Strains and Chemicals

The *S. cerevisiae* reporter strain FE440[23] expressing a green fluorescent protein (GFP) controlled by the ribosomal protein RPL22a promoter and thus correlated to growth was mainly used throughout this study. The ethanol reporter strain Sc-PCK1-B (Johansen et al. (2013), unpublished) expressing a blue fluorescent protein (BFP) controlled by the phosphoenolpyruvate carboxykinase promoter and thereby correlated to ethanol growth/non glucose growth (glucose repression/derepression) was used for a few cultivations. All chemicals used during the study were obtained from Sigma Aldrich (St. Louis, USA).

Cultivation conditions

Pre-culture. A single colony of the growth reporter FE440 respectively the ethanolapplied reporter strain Sc-PCK1-B was picked from a plate with minimal medium and used to inoculate a 0.5 L baffled shake flask with 100 ml of defined mineral medium containing 7.5 g/L $(NH_4)_2SO_4$, 14.4 g/L KH_2PO_4, 0.5 g/L $MgSO_4*H_2O$, 2 ml/L trace metal solution, 1 ml/L vitamin solution and 10 g/L glucose[24]. The pre-culture was incubated in an orbital shaker set to 150 rpm at 30°C until mid-exponential phase (approximately 10 h) and directly used for inoculation.

Chemostats. One compartment: Aerobic level-based chemostats were run with the growth reporter strain FE440 in 1 L bioreactors (Sartorius, B. Braun Biotech International, GmbH, Melsungen, Germany). pH and DOT electrodes (Mettler Toledo, OH, USA) were calibrated using two point calibrations. The pH was kept constant at 5.0 using 2 M NaOH. Temperature, aeration and stirring were kept constant at 30° C, 1 v/vm and 600 rpm, respectively. The OD_{600} for inoculation was 0.001. The growth medium was a defined mineral medium according to Verduyn *et al.* (1992)[24] with 5 g/L glucose for the batch phase. A factorial design was used for the continuous mode with glucose concentrations in the feed of 50 g/L or 300 g/L and the dilution rates of D = 0.05 and 0.2 h^{-1} The experiments were performed in duplicate. In addition a center point cultivation was included with D = 0.125 h^{-1} and 125 g/L glucose.

Two compartments: A 5 L reactor (V_2) connected to a 0.5 L reactor (V_1) (Sartorius, B. Braun Biotech International, GmbH, Melsungen, Germany) was used with a ratio of the working volume of $V_1 = 1/6*V_2$ (figure 1). V_1 hereby represented the feeding zone with feed addition and no sparging of oxygen whereas V_2 corresponded to the remaining reactor volume. The 5 L reactor contained the outlet of the system and was sparged with oxygen. Between the two reactors a recirculation was applied (F_1 and F_2). Running conditions were the same as for the

one-compartment chemostats, described above. Aerobic level-based chemostats with different overall dilution rates (D = 0.05 and 0.2 h^{-1} as well as D = 0.125 h^{-1} as center point, calculated for the whole reactor volume of the setup), glucose feed concentration (50 g/L, 125 g/L and 300 g/L) and recirculation flow (F_2 = 0.1 L/h, 1.45 L/h and 3 L/h) between the two reactors were performed for selected conditions according to a factorial design experiment plan (see table 1).

For both setups, the one- and two-compartment setup, the batch phase was followed by OD_{600} measurement and continuous analysis of the off-gas composition by a Mass spectrometer (Prima Pro Process MS, Thermo Fisher Scientific, Winsford UK). After glucose depletion, detected as a rapid drop in the CO_2 content of the off gas, the cultures were switched to chemostat mode with the desired dilution rate by applying a feed with the same medium as used for the batch but containing 50 g/L, 125 g/L respectively 300 g/L glucose . The volume was kept constant by a level based outlet for both the one- and two-compartment experiments. Steady state was considered established when dry weight, dissolved oxygen tension (DOT), metabolites and exhaust gas concentration (CO_2) had remained constant for at least three residence times. For the ethanol reporter strain, and additional fed-batch phase was integrated into the process after glucose depletion to validate if the same steady state was reached as when the continuous mode was started with a lower biomass concentration after the batch. Therefore, a feed with 300 g/L glucose at a growth rate of 0.1 h^{-1} was applied until a biomass concentration of 25 g/L was reached.

Samples were withdrawn for OD_{600}, high performance liquid chromatography (HPLC), dry weight (DW) and flow cytometry analysis. Samples for OD_{600} and DW were analyzed directly, HPLC samples were sterile filtered and stored at -20 °C. Samples for flow cytometry were mixed with glycerol to a final concentration of 15 % and frozen and stored in a -80°C

freezer. The sampling frequency was once every residence time until the 9th residence time starting with the 0th residence time directly after switching to chemostat mode, as well as three samples during exponential growth in batch mode. For the one-compartment experiments samples where withdrawn at the outlet whereas for the two-compartment experiments samples were additionally withdrawn from both outlets of the recirculation lines (V_1 and V_2, see figure 1, marked with an arrow).

Sample analysis

OD, DW and HPLC. Growth was monitored by measuring OD_{600} with a Shimadzu UV mini 1240 spectrophotometer (Shimidzu, Kyoto, Japan). Dry weight measurements were performed on 5 mLl cultivation broth according to Olsson and Nielsen (1997)[25]. The concentrations of glucose, acetate, ethanol, glycerol and pyruvate in the broth were determined by HPLC as earlier described by Carlquist *et al.* (2012)[23].

Flow cytometry. A FACSAria™ III (Becton-Dickinson, NJ, USA) flow cytometer was used for single-cell analysis ofboth yeast and bacteria. Excitation wavelength for the laser was set to 488 nm. Two scattering channels (FSC and SSC) and two fluorescent detection channels were used in the analysis. Fluorescence emission levels were measured using a band pass filter at 530±30 nm for GFP and 450±20 nm for BFP. Light scattering and fluorescence levels were standardised using 2.5 µm fluorescent polystyrene beads. Samples for flow cytometry were centrifuged for 1 min at 3000 g and 4 °C, resuspended in 0.9 % saline solution and directly analysed. 10,000 yeast cell events were recorded for yeast. CS&T beads (Cytometer Setup and Tracking beads) (Becton Dickinson, USA) were used for the automated QA/QC of the machine performance.

Data analysis

Processing and analysis of the flow cytometry raw data was performed using MatLab ® R2013a (The MathWorks, Inc., Natick, MA, USA). The raw data was extracted from the flow cytometer as fcs files and loaded into MatLab with the help of the readfsc function (by L. Balkay, University of Debrecen, Hungary, available on MatLab central file sharing). The HPLC data were imported from excel. The data from the fcs files was saved into mat files including the recorded GFP fluorescence and the FSC for each experiment. By application of the hist function to the 1024 recording channels cell count was saved for all channels and histogram plots generated. For better quantitative description of the GFP distributions, the mean function was used to calculate the mean FSC and mean GFP fluorescence. By dividing the standard deviation of the GFP distribution by the mean GFP the coefficient of variance (CV) of the distribution was generated.

Modeling Aspects

A two-stage PBM (population balance model) previously developed for a batch cultivation[1] was adapted to describe a continuous cultivation in a one- and two-compartment setup (see figure 1). Cell total protein content (a measure of cell size) is used as model variable. In the case of the two-compartment setup presented in this work, four population balance equations are necessary (two cell stages x two compartments). Furthermore, the dilution terms taking into account the transport between compartments, inlet and outlet are included in the PBM equations for both the case of the one- and the two-compartment models. The PBM equations for a two-compartment model are presented in Appendix 1 (Eq. A1-1 to A1-4). For further details on the formulation of a PBM and the various model kernels forming the PBM equations, the paper by Lencastre Fernandes *et al.,* (2013)[1] should be consulted. The same boundary and initial conditions as proposed for the batch cultivation model are used for both compartments.

Based on the trajectory of the estimated critical sizes along a batch cultivation[1] the budding and division critical sizes were defined as continuous functions of the concentrations of glucose or ethanol, in a given compartment, according to the following assumptions:

- If the concentration of glucose, in a given compartment, is equal to or above 0.1 g/L, growth on glucose is assumed for that compartment, and the critical budding (μ_B) and division (μ_D) sizes are calculated based on the glucose concentration according to Eq. A1-6 to A1-7 in Appendix 1
- If the concentration of glucose, in a given compartment, is below 0.1 g/L, growth on ethanol is assumed for that compartment, and the critical budding (μ_B) and division (μ_D) sizes are calculated based on the glucose concentration according to Eq. A1-8 to A1-9 in Appendix 1
- If the concentrations of glucose and ethanol, in a given compartment are below $1e^{-6}$ g/L, growth in that compartment is assumed to be zero. An estimated value for the saturation constant of the overall growth process (corresponding to half of the maximum specific growth rate) is 0.15 g/L[26].
- The partition shape parameters (necessary for defining the birth kernel in the PBM equations) are assumed to change according to the growth mode (glucose or ethanol) observed in a given compartment: for glucose growth, $\alpha=\beta=50$, for ethanol growth $\alpha=30$ and $\beta=60$. The nature of these values is further discussed in Lencastre Fernandes *et al.* (2013)[1].

In order to further describe the bulk concentration of glucose, ethanol and oxygen in the cultivation media, in each compartment, an unstructured model was coupled to the PBM (see Eq. A1-10 to A1-15). As presented for the experimental setup (see figure 1), the glucose feed is added to the inlet of compartment one, and the oxygen supply takes place exclusively in

compartment two. As proposed for the batch model[1], the substrate dependent term in the growth kernel ($\lambda(Z)$) is evaluated, in this case, for each of the compartments (see Eq. A1-16).

The model was implemented and solved in MatLab® Release R2013a, and the fixed-pivot method was used for discretization of the PBM equations. The unstructured and PBM models are solved iteratively, following a solution procedure similar to the one proposed for the batch model[1].

Results and discussion

The model simulations, basically extending the model results from batch experiments[1] to continuous one- and two-compartment setups, were performed first, in order to identify the most interesting experiments, which were then carried out in the laboratory.

***In silico* simulations of the two-compartment, scale-down system**

Simulations with the model (details see materials and methods as well as appendix 1) were performed. Different operating conditions were evaluated *in silico* using a factorial design plan (table 1) varying glucose feed concentration (either 50 g/L, 125 g/L or 300 g/L which is referred to in the text as G_{50}, G_{125} respectively G_{300}), dilution rate (D = 0.05 h^{-1}, 0.2 h^{-1} and a center point corresponding to D = 0.125 h^{-1} (referred to as $D_{0.05}$, $D_{0.2}$ and $D_{0.125}$)) as well as recirculation between the two reactor compartments (low recirculation (LR) = 0.1 L/h, medium recirculation (MR) = 1.45 L/h, high recirculation (HR) = 3.0 L/h). Hereby, the choice of conditions was based on the intention to test the two-compartment model under extreme conditions to evaluate the borders of applicability. For the one-compartment cultivation simulations, steady state was found for all conditions apart from case F (G_{50}_$D_{0.05}$), G (G_{50}_$D_{0.05}$) and H (G_{50}_$D_{0.2}$) for which oscillations, particularly visible in the oxygen concentration and budding index, were observed. Furthermore, for case E (G_{50}_$D_{0.05}$),

F ($G_{50}\_D_{0.2}$) and G ($G_{50}\_D_{0.05}$) smaller cell sizes than for the other conditions were predicted because only residual concentrations of glucose and ethanol remained. In contrast to that, larger cell sizes were observed for case B ($G_{300}\_D_{0.2}$), C ($G_{300}\_D_{0.05}$) and D ($G_{300}\_D_{0.2}$), because these cases showed the highest glucose concentration in steady state. For the two-compartment simulations, as expected, it was obvious that a lower recirculation resulted in larger differences between the two compartments, which could particularly be seen for case B ($G_{300}\_D_{0.2}\_LR$) where the largest difference in oxygen concentration between the two compartments was found. Moreover, for the cases C ($G_{300}\_D_{0.05}\_HR$), G ($G_{50}\_D_{0.05}\_HR$) and E ($G_{50}\_D_{0.05}\_LR$) ethanol consumption was predicted to take place in compartment V_2, because glucose concentrations were below 0.1 g/L and the model contains a switch to ethanol consumption when the glucose concentration goes below the 0.1 g/L threshold. Furthermore, as for the one-compartment model, oscillations were found for the cases A ($G_{300}\_D_{0.05}\_LR$), H ($G_{50}\_D_{0.2}\_HR$) and I ($G_{125}\_D_{0.125}\_MR$) with momentaneous low glucose, ethanol and oxygen concentrations during the oscillation periods.

The continuous cultivation scale-down reactor system

To mimic the gradients often seen in large-scale cultivations and the consequent development of compartments with different microenvironments inside a reactor which influence the microbial population behavior, a two-compartment reactor setup was constructed (figure 1). Similar to the model, the experimental setup consists of two reactors with a volume ratio 1:6. The smaller reactor (V_1) represents the feeding zone with feed addition (glucose concentration in the feed was either 50 g/L, 125 g/L or 300 g/L) and no sparging of oxygen, whereas the bigger reactor (V_2) corresponds to the remaining reactor volume containing the outlet, considerably lower glucose concentration and sparging with oxygen (figure 1). A circulation loop (with flow F_1 and F_2, respectively) ensured the exchange between the two

reactors, where the recirculation from V_2 to V_1 (F_2) was varied according to the factorial design plan (table 1; low recirculation (LR) = 0.1 L/h, medium recirculation (MR) = 1.45 L/h, high recirculation (HR) = 3.0 L/h). Overall dilution rates (calculated for the whole working volume of both reactors) of D = 0.05 h^{-1} and 0.2 h^{-1} (referred to as $D_{0.05}$ and $D_{0.2}$), in addition to a center point corresponding to D = 0.125 h^{-1} (referred to as $D_{0.125}$) were applied. Due to the volume differences and circulation between the reactors (two compartments) with only one feed inlet, the actual dilution rates in the two compartments and local dilution rates in the compartments can be higher than what is normally possible without experiencing a wash-out of biomass.

On the basis of the simulation results, selected conditions were performed experimentally (table 1). These included two cases (G_{300}_$D_{0.05}$_LR (A) and G_{50}_$D_{0.05}$_LR (E)) run with D = 0.05 h^{-1} and 50 g/L respectively 300 g/L of glucose feed both with low recirculation flow rate between the reactors. Furthermore, to be able to evaluate the effect of a higher overall dilution rate on the cell population structure, also cases F and H (G_{50}_$D_{0.2}$_LR respectively _HR), corresponding to a low and high recirculation flow rate respectively, were included in the experimental study. In the case H (G_{50}_$D_{0.2}$_HR) oscillations were found when performing simulations as well as for the center point (case I) which was also chosen to be carried out as a middle-range condition between the extremes (G_{125}_$D_{0.125}$_MR). In addition to the comparison of the model and the two-compartment setup, all experimental results are also compared to the corresponding one-compartment chemostat experimental cultivation and model simulation.

Variation of general physiology over time in the two-compartment setup

When comparing the general physiology between the modeling and experimental results in the two-compartment setup, all experimentally performed cases achieved a steady-state,

which was not seen for all modeling results, though after a different number of residence times depending on the conditions (figure 2).

For growth at the high dilution rate, D= 0.2 h^{-1} (cases F (G_{50}_$D_{0.2}$_LR) and H (G_{50}_$D_{0.2}$_HR)), the cells generally consumed the fed glucose producing CO_2 and ethanol due to overflow metabolism. When the experiment was performed with low recirculation flow rate (case F (G_{50}_$D_{0.2}$_LR), figure 2) a high rest glucose concentration was observed in compartment V_1, around half of the concentration in the feed, along with low amounts of produced biomass (end value for biomass concentration: around 3 g/L). The dilution rate in compartment V_1 was much higher than the overall dilution rate as the incoming feeding rate was based on the overall volume of the two reactors (3.5 L) and V_1 only comprises 1/7 of the total volume. This implies that cells, glucose and ethanol were transported to V_2. In this compartment the incoming glucose was readily consumed and ethanol accumulated (ethanol concentration was around 3 g/L), resulting in a clear compartmentalization of the scale-down system. The model simulations supported these observations (figure 3), and further suggested that cells in V_2 had not switched to ethanol growth: a high budding index (around 60%) was predicted for both compartments, and the predicted cell size distributions were similar, although slightly smaller cells were observed in V_2 as expected on the basis of earlier studies[27,28] because lower glucose concentrations were observed. No other metabolites were found in significant amounts in any of the compartments.

When applying a high recirculation flow rate between the compartments (case H (G_{50}_$D_{0.2}$_HR)), both compartments exhibited the same concentration profiles (figure 2). This was expected and predicted by the model simulations (figure 3), as the high exchange between compartments brings the system closer to the one-compartment case (i.e. where ideal mixing and homogeneity in the reactor is assumed). This makes this case less interesting for detailed studies in the scale-down setup. The glucose fed to V_1 was readily consumed, CO_2

was produced as well as small amounts of biomass (around 12 g/L) and ethanol (around 5 g/L). In the model simulations an oscillatory behavior was observed, in particular for the budding index profile for both compartments and for the oxygen profile for compartment V_2. These oscillations are a result of a continuous shift between glucose and ethanol growth modes, since the budding and division critical sizes (and consequently the growth rate) decrease gradually following the glucose concentration. When the glucose concentration reaches the threshold value, the partition shape parameters change resulting in the generation of new smaller cells, which grow slower leading to an accumulation of glucose and when the glucose concentration again rises above the threshold value the shape parameters change once again leading to an accumulation of bigger cells and thus a faster growth rate and faster consumption of glucose (leading to a decrease of the glucose concentration). These oscillations were not visible in the experimental results. It remains to be determined whether the oscillations are exclusively due to a model artifact (due to the assumptions that were made) or they take place in reality, but the frequency of the experimental sampling applied here was too low to capture this phenomenon.

When lowering the dilution rate to D = 0.125 h^{-1} and elevating the glucose feed concentration to 125 g/L (case I, center point, G_{125}_$D_{0.125}$_MR), a similar picture as for the high dilution rate (case H, G_{50}_$D_{0.2}$_HR) was observed (figure 2). Whereas there was no difference in biomass concentration between the two compartments (up to around 25 g/L), the ethanol level was different, which revealed some differences compared to a one-compartment setup, and therefore makes this condition more interesting to investigate further compared to case H (G_{50}_$D_{0.2}$_HR). The fed glucose was readily consumed in compartment V_1 producing CO_2, biomass and ethanol (around 25 g/L). The remaining glucose and ethanol were recirculated and completely consumed in the compartment V_2. The model simulation also predicted oscillations for this case (figure 3).

For experiments with the low dilution rate (D = 0.05 h^{-1}, cases A (G_{300}_$D_{0.05}$_LR) and E (G_{50}_$D_{0.05}$_LR)) the fed glucose was only partly consumed in V_1 producing ethanol, CO_2 and biomass (figure 2). The remaining glucose, the formed ethanol and biomass were transported into V_2, where significantly higher biomass concentrations were detected. When increasing the feed glucose concentration, an increase in the produced biomass concentration (to around 50 g/L vs 20 g/L), ethanol concentration (around 20 g/L vs 5 g/L) and CO_2 were observed in both compartments, as well as a higher remaining glucose concentration in V_1. In contrast to experiments with lower glucose concentration, also small amounts of glycerol were detected in V_1 for case A (G_{300}_$D_{0.05}$_LR).

Whereas the model predictions for case E (G_{50}_$D_{0.05}$_LR) were in agreement with the experimental results, the model predictions for case A (G_{300}_$D_{0.05}$_LR) were not (figure 3). Indeed, while the model only predicted a very low glucose concentration in V_1 for case A, a significant amount of glucose was observed after 6 retention times in the experiments. It is however not clear if a steady state has been reached at that point or if a further decrease of the glucose concentration (to residual levels) would be observed when continuing the cultivation. An explanation for this could be that the cells are more stressed due to the high glucose concentration, and hence need longer time to adjust and to reach steady state. It could be a similar phenomenon as seen in high gravity batch cultivations, where a lag phase/phase of slow growth of about 20 h is seen before the exponential growth phase starts[29]. This was not incorporated in the model, as the model did not take into account high-gravity cultivations, and could thereby lead to different simulation results compared to the experiments.

The effect of compartmentalization on biomass productivity and yields on substrate

It is obvious from the previous section that the degree of compartmentalization, here determined by the exchange flow rate between compartments, as well as growth rate and feed concentration in a bioreactor have a significant influence on cell physiology. Therefore, it is

also interesting to investigate the effect of compartmentalization on the overall yields on glucose as well as on the productivity of biomass in the experimentally performed cases (figure 4). Hereby only the yields of biomass, ethanol and CO_2 were considered because other metabolites produced in low amounts like acetate, glycerol and pyruvate only accounted for less than 10% in the carbon balance (data not shown). This is consistent with Postma *et al*. (1989)[31] who found that below D= 0.25 h^{-1} no other byproducts than ethanol were accumulated.

The biomass yields for one- and two-compartment continuous cultivation differed significantly. In general, the biomass yields (figure 4A) and thereby also the biomass productivity (figure 4D) for the two-compartment cultivations were around 50% higher than for the ordinary chemostat cultures, except for case E (G_{50}_$D_{0.05}$_LR) where the opposite was found. The highest, respectively, lowest productivity was found for case F and H (G_{50}_$D_{0.2}$) respectively case E (G_{50}_$D_{0.05}$) in one-compartment chemostats. In the two-compartment setup case A (G_{300}_$D_{0.05}$_LR) showed the highest productivity and case E (G_{50}_$D_{0.05}$_LR) again the lowest productivity. In general, the values found for the two-compartment setup, although differences in oxygen level might exist, were comparable with biomass yields seen in earlier studies in ordinary chemostats by e.g. van Dijken *et al.* (2000)[32] whereas for the one-compartment setup values were lower than reported in earlier studies. The ethanol yields (figure 4B) were in all experimentally performed cases around three-fold higher for the one-compartment chemostats than for the two-compartment setup with the exception of case E (G_{50}_$D_{0.05}$_LR) for which the yields were almost the same in both setups. Also for the CO_2 yields (figure 4C) the one-compartment chemostats showed higher values than for the two-compartment cultivations, with the exception of case A (G_{300}_$D_{0.05}$_LR) for which the yield was around three times higher for the conventional chemostat. In general, no clear dependence of the yields on the dilution rate could be observed. When increasing the

recirculation rate in the two-compartment setup, it is expected that the yields should increasingly resemble the one-compartment chemostat, which could not be seen from the results. In fact, in the results only the CO_2 yield decreased, whereas the biomass yield increased when comparing low and high recirculation rate (case F and H, G_{50}_$D_{0.2}$_LR respectively _HR). An increase in glucose feed concentration (comparing case A (G_{300}_$D_{0.05}$_LR) and E (G_{50}_$D_{0.05}$_LR)), however, resulted in a decrease in biomass yield as well as an increase in CO_2 yield for the two-compartment, respectively, decrease for the one-compartment chemostat. In large-scale cultivations of *S. cerevisiae* it has been found that when cells experience a fast change in environmental conditions[34], the biomass yield decreases in line with an increase in ethanol yield. The reason for this are microenvironments in different parts of the bioreactor due to non-ideal mixing, which also makes cells more stressed, as determined by the expression of stress related genes[15]. This explains the observed decrease in biomass concentration when the feed concentration increased, since this imposes a larger difference in environment between the two compartments. However, the increase in ethanol yield was only seen for the one-compartment chemostat, whereas it remained constant in the scale-down setup.

Cell size distributions in the two-compartment setup

The cell size distribution changed depending on the conditions when comparing the two compartments in the model as well as the experiments (figure 5 and 6), and also in comparison with ordinary chemostat cultivations (figure 10 and Appendix 2). For the experimental cases with low respectively medium dilution rate and recirculation (A (G_{300}_$D_{0.05}$_LR), E (G_{50}_$D_{0.05}$_LR) and I (G_{125}_$G_{0.125}$_MR)) the cell size remained the same for cells in both compartments as well as cells grown in a normal chemostat (one-compartment cultivation): 338.43±+/-0.56 vs 338.12±+/-30.63 vs 354.59±+/-5.48. This is in

agreement with the model predictions for case E (G_{50}_$D_{0.05}$_LR) and I (G_{125}_$D_{0.125}$_MR), though for case I (medium dilution rate) two different size subpopulations were predicted, which in the experimental results can only be suspected (figure 6). The differently sized subpopulations seen in the model simulations are possibly related to oscillations in cell size and budding index originating from the switch between glucose and ethanol growth being set to take place at a discrete glucose concentration of 0.1 g/L, resulting in smaller cells during ethanol growth and bigger cells during growth on glucose. For case A (G_{300}_$D_{0.05}$_LR) the model predictions, however, suggested that two different cell size distributions would be observed in the two compartments: a smaller sized population is predicted for V_2, while a combined population of smaller and bigger cells would be found in V_1 (see table 2). This difference between experimental and model predictions is consistent with the discrepancies found for the physiological data, and thus further suggests that the model may not be suitable for describing high-gravity cultivations. But it also has to be mentioned that high-gravity cultivations were not explicitly considered during the model development. However, the smaller cell size could be explained by a change in osmolarity, as it was found earlier that incrasing osmolarity leads to shrinking cells[30].

For cases with high dilution rate and low respectively high recirculation (F and H, G_{50}_$D_{0.2}$_LR respectively HR) experimental cell size data for case F (G_{50}_$D_{0.2}$_LR) showed similarities to case E (G_{50}_$D_{0.05}$_LR) but with higher mean cell size, whereas for case H (G_{50}_$D_{0.2}$_HR) the cell size distribution resembled more case A (G_{300}_$D_{0.05}$_LR) and I (G_{125}_$D_{0.125}$_MR) (figure 5). The model predicted two differently sized populations for case H (G_{50}_$D_{0.2}$_HR), as for case I (G_{125}_$D_{0.125}$_MR) as discussed above, which might be explained by the higher applied recirculation flow rate between the two compartments (figure 6).

The model predictions for case F (G_{50}_$D_{0.2}$_LR) revealed different distributions in comparison to case A (G_{300}_$D_{0.05}$_LR), H (G_{50}_$D_{0.2}$_HR) and I (G_{125}_$D_{0.125}$_MR) as well: smaller size populations were predicted for these cases, reflecting the shift of the population in response to a lower glucose concentration (figure 6). As previously discussed, for these cases higher glucose concentrations were measured in comparison to the model predictions, which was in agreement with the experimentally measured distributions displaying larger cells than shown in the predicted distributions.

In comparison with the one-compartment model (see appendix 3, figure 13) cell size distributions predicted for cases with low recirculation (A (G_{300}_$D_{0.05}$_LR), E (G_{50}_$D_{0.05}$_LR) and F (G_{50}_$D_{0.2}$_LR)) resembled distributions found in the two-compartment model for V_2, which seems to be expected as the biggest part of the one-compartment chemostat will resemble the compartment V_2 with high oxygen concentration and residual glucose concentration. For cases with high respectively medium recirculation (H (G_{50}_$D_{0.2}$_HR) and I (G_{125}_$D_{0.125}$_MR)), cell size distributions in the one-compartment model resembled the subpopulation that showed the higher cell size in the two-compartment model, probably due to less changes in the residual glucose concentration predicted in the one-compartment reactor.

The results suggest that the lowest level of population heterogeneity resulted from the operating conditions corresponding to the lowest local dilution rates (case E (G_{50}_$D_{0.05}$_LR), table 2). Oppositely, the highest level of population heterogeneity was found for case H (G_{50}_$D_{0.2}$_HR), where the highest local dilutions rates compared to the overall dilution rate should be observed. This suggests that a high local volume exchange contributes significantly to the heterogeneity of the cell population. A high glucose feed concentration is likely to be an additional factor contributing to a higher level of heterogeneity.

Influence of compartmentalization on cell membrane robustness

To gain further physiological information about how compartmentalization affects the yeast population, a *S. cerevisiae* reporter strain expressing a green fluorescent protein (GFP) under the control of a ribosomal promoter was applied[23]. This strain has earlier been demonstrated to be a useful tool to follow growth characteristics at single cell level. Additionally, when exposing the cells to freeze-thaw stress, the reporter strain can be applied for the investigation of cell membrane robustness, as a strong correlation between intracellular GFP level and cell membrane robustness has been found[23]. Hence this strain functions as a dual reporter and is a good model system for investigating how different environmental conditions may affect microbial responses and stress tolerance on single-cell level. All performed experimental cases except of case G_{50}_$D_{0.2}$_HR, (H) where no physiological difference between the compartments could be established, were investigated for single cell membrane robustness in one- and two-compartment chemostats.

Flow cytometry analysis was applied on frozen cells from two subsequent retention times, and from the resulting fluorescence distributions it can be seen that for all cases steady state of the fluorescence level was established (figure 7). A clear difference in GFP fluorescence between the compartments could only be seen for cultivation G_{50}_$D_{0.05}$_LR (case E), where compartment V_1 displayed two subpopulations, whereas only one major population was seen for compartment V_2 (figure 7). For the remaining experiments, the calculated mean fluorescence differed less than 10% between compartments (table 3), although the general physiology in the two compartments was different for cases with low recirculation rate, i.e. in addition to case E (G_{50}_$D_{0.05}$_LR) also for case A (G_{300}_$D_{0.05}$_LR). The reason for this discrepancy is probably the longer expression time of GFP compared to the recirculation time between the two compartments.

However, fluorescence distributions can still be compared between all cases. Case A (G_{300}_$D_{0.05}$_LR), F (G_{50}_$D_{0.2}$_LR), I (G_{125}_$D_{0.125}$_MR) and compartment V_2 of case E (G_{50}_$D_{0.05}$_LR) exhibited similar steady state characteristics with a broad distribution tailing towards lower fluorescence (figure 7), although the tailing was less obvious for cells growing at the higher dilution rate, which can be seen in the slightly higher mean fluorescence values found for the higher dilution rate compared to experiments performed with D = 0.05 h^{-1}. Furthermore, this was also illustrated by lower CV for the GFP distribution for cells cultivated at higher dilution rate, which were in the range 0.23-0.26 compared those cultivated at lower dilution rate, which were in the range 0.41-0.56). These findings directs towards the conclusion, that the membranes of cells growing with higher dilution rate seems to be more robust towards freeze-thaw stress, whereas cells growing at lower dilution rate are generally more affected. This is interesting since generally it is found that in continuous culture cells growing at a low dilution rate are more robust and tolerant to stress than cells growing with a higher growth rate[35,36]. This trade-off between growth rate and stress tolerance is believed to be connected to energy availability. As stated above, compartment V_1 of case E (G_{50}_$D_{0.05}$_LR) revealed two subpopulations, one high fluorescent containing around 65% of the whole population and one low fluorescent (around 35% of the population). Hence, in this compartment a subpopulation of cells showed decreased membrane robustness compared to the rest of the cell population as well as the majority of the cells in compartment V_2 under conditions applied in case E.

In comparison to steady state values of ordinary chemostats (Appendix 2, figure 11), the two-compartment cultivations revealed generally lower mean fluorescence values (table 3). This indicates that cells grown in one-compartment chemostats are less affected by freeze-thaw stress than cells grown in a two-compartment chemostat. Only when growing with D = 0.05 h^{-1} in an ordinary chemostat (case A (G_{300}_$D_{0.05}$) and E ($G_{300}G_{50}$_$D_{0.05}$)), a small portion of

the cell population seemed to be strongly affected by freeze-thaw stress and the influence became stronger with higher glucose concentration in the feed. For the same conditions in a two-compartment chemostat highly effected cells were only found for case E (G_{50}_$D_{0.05}$ LR) in compartment V_1, whereas no subpopulations were found for case A (G_{300}_$D_{0.05}$_LR), but the same general trend for the feed concentration was seen.

Influence of compartmentalization on ethanol/glucose consumption

To further investigate physiological differences between the two compartments of the scale-down setup and differences compared to a one-compartment chemostat, an ethanol reporter strain (Johanson, unpublished) was cultivated in the system with a dilution rate of D = 0.2 h^{-1}, 50 g/L glucose feed concentration and low recirculation between the two compartments (experiment G_{50}_$D_{0.2}$_LR case F). This condition was chosen because it revealed clear differences in ethanol and glucose level between the two compartments. Additionally, the ethanol concentrations in the two-compartment setup were much lower than seen for an ordinary, one-compartment chemostat (figure 8). The strain expresses a blue fluorescent protein (BFP), whose expression is controlled by the PCK1 (phosphoenolpyruvate carboxykinase 1) promoter. The promoter regulates the expression of a key enzyme of gluconeogenesis, is repressed when glucose is present and active during growth on ethanol. Consequently, the BFP fluorescence can be correlated to growth on ethanol.

Cells cultivated in an ordinary, one-compartment chemostat having the same dilution rate and glucose feed concentration expressed very low levels of fluorescence (mean BFP 65.88±+/-6.04, figure 8), and hence no growth on ethanol took place in this setup. In comparison, the mean BFP fluorescence in the two-compartment cultivation was about 64 % higher, and additionally, a higher degree of heterogeneity (coefficient of variance (CV) of the

distributions: V_1: 0.65 respectively V_2: 0.50 vs. one-compartment: 0.35), characterized by a broader and less aligned distribution, was generally seen. However, almost no difference in the BFP fluorescence level of the ethanol reporter could be recognized for the two compartments (mean fluorescence: V_1: 191.25±10.12 respectively V_2: 170.84±+/. 26.88) over three residence times (figure 8). Only small shape differences in the main part of the fluorescence distribution were found, which influenced the mean fluorescence. The fluorescence during the two-compartment cultivation was around half of the value observed for ethanol growth in batch cultivations. These findings, in addition to the differences in ethanol and biomass concentrations, both between the compartments and compared to the one-compartment setup, indicate that cells in the two-compartment system utilize ethanol as glucose repression is released, particularly in V_2, were no feeding was applied. However, in comparison to the recirculation rate, the degradation of BFP fluorescence as well as possibly also the release of glucose repression are too slow, and as a consequence a switch from PCK1 repression to expression cannot be directly captured by the fluorescence from the reporter strain, rather an average value representing the time cells spend under glucose excess versus glucose starvation conditions is registered. It could be interesting to perform two-compartment cultivations with even slower recirculation flow rate, to verify whether differences in BFP expression between compartments can be detected. Nonetheless it was demonstrated that the two-compartment setup is beneficial to investigate characteristics in cellular responses related to concentration differences between the feeding zone and the remaining reactor volume and the flows between compartments, which cannot be captured using a conventional chemostat. Consequently, by applying the here developed scale-down system the expression differences cells exhibit in different parts of a large-, industrial-scale reactor can be simulated experimentally[9].

Conclusion and general applicability of approach for future experiments

The here presented approach of modeling in combination with the performance of experimental work showed consistency or at least the same trend in most cases but also limitations, especially under extreme growth conditions (high gravity glucose cultivations). In general, though, the approach is still useful for process optimization by applying modeling to get an overview of conditions that might be interesting to perform in lab-scale experiments exhibiting special traits like e.g. oscillations found during our simulations. Such an approach can reduce the amount of experiments to be performed because conditions revealing standard characteristics in the model might not need to be performed in the lab. One thing that remains to be done in the future, on the basis of the available data, is to refine the model further such that the predictive ability of the model for the two-compartment set-up is improved, also for high gravity cultivation conditions.

The experimental setup can be used for studies of production processes in the development phase for e.g. recombinant proteins, to investigate how production is influenced by compartmentalization at different conditions. Furthermore, by applying reporter strains the single cell response e.g. in stress genes, growth or ethanol growth in the different compartments can be studied. For this purpose it could also be interesting to include more sampling points or study more different recirculation times and dilution rates to test the operating limits of the setup. In comparison to pulse experiments in conventional chemostats, a setup like the one presented here has the advantage that the flows between the two compartments are known, which makes it possible to assess phenomena like the ones seen for the ethanol reporter strain. Furthermore, in this setup the repeated exposure of cells to a changing environment is taken into account whereas in perturbation studies this is only achieved by pulsed feed experiments, which are rarely reported up to now in physiological investigations of single cells[37]. Compared to a setup with a STR connected to a PFR, the here

presented setup provides a steady state environment which is simplifying the overall picture in the reactor and is not found in a PFR as conditions are changing with further proceeding in the reactor away from the feeding point. Furthermore, the second STR also provides a distribution of cell properties, which might be closer to the real scenario in a large production tank as cells rarely experience a strict gradient. Though using a PFR instead of the second STR allows sampling in a more controlled environment to see changes over time, which helps to investigate isolated phenomena, rather than an interplay of multiple happenings in a bioreactor. The Recirculation in these systems can also be set to give shorter mixing times.

Acknowledgement

The Danish Council for Strategic Research is gratefully acknowledged for financial support in the frame of the project "Towards robust fermentation processes by targeting population heterogeneity at microscale" (project number 09-065160). ERA-IB (ERA-NET Industrial Biotechnology) is gratefully acknowledged for financial support in the frame of the project "Targeting population heterogeneity at microscale for robust fermentation processes" (project number EIB.08.031).

References

1. Lencastre Fernandes R, Carlquist M, Lundin L, Heins A-L, Dutta A, Sørensen SJ, et al. Cell mass and cell cycle dynamics of an asynchronous budding yeast population: experimental observations, flow cytometry data analysis, and multi-scale modeling. *Biotechnol Bioeng*. **110**(3):812–26 (2013).

2. Müller S, Harms H, Bley T. Origin and analysis of microbial population heterogeneity in bioprocesses. *Curr Opin Biotechnol.* **21**(1):100–13 (2010).

3. Koutinas M, Kiparissides A, Pistikopoulos EN, Mantalaris A. Bioprocess systems engineering : transferring traditional process engineering principles to industrial biotechnology. *Comput Struct Biotechnol*. **3**(4): 1-9 (2012).

4. Ferrer-Miralles N, Domingo-Espín J, Corchero JL, Vázquez E, Villaverde A. Microbial factories for recombinant pharmaceuticals. *Microb Cell Fact*. **8** (17): 1-8 (2009).

5. Chemler J, Yan Y, Koffas MG. Biosynthesis of isoprenoids, polyunsaturated fatty acids and flavonoids in *Saccharomyces cerevisiae*. *Microb Cell Fac* **5** (20): 1-9 (2006).

6. Larsson G, Törnkvist M, Wernersson ES, Trägårdh C, Noorman H, Enfors S-O. Substrate gradients in bioreactors: origin and consequences. *Bioprocess Eng*. **14**(6):281–9 (1996).

7. Schweder T, Krüger E, Xu B, Jürgen B, Blomsten G, Enfors SO, et al. Monitoring of genes that respond to process-related stress in large-scale bioprocesses. *Biotechnol Bioeng*. **65**(2):151–9 (1999).

8. Vrabel P, Lans RGJM Van Der, Luyben KCAM, Boon L, Nienow AW. Mixing in large-scale vessels stirred with multiple radial or radial and axial up-pumping impellers□: modelling and measurements. *Biotechnol Bioeng*. **55**:5881–96 (2000).

9. Bylund F, Collet E, Enfors S-O, Larsson G. Substrate gradient formation in the large-scale bioreactor lowers cell yield and increases by-product formation. *Bioprocess Eng*.**18**(3):171-180 (1998).

10. Enfors SO, Jahic M, Rozkov A, Xu B, Hecker M, Jürgen B, et al. Physiological responses to mixing in large scale bioreactors. *J Biotechnol*. **85**(2):175–85 (2001).

11. Lidstrom ME, Konopka MC. The role of physiological heterogeneity in microbial population behavior. *Nat Chem Biol*. Nature Publishing Group, **6**(10):705–12 (2010).

12. Lara AR, Leal L, Flores N, Gosset G, Bolívar F, Ramírez OT. Transcriptional and metabolic response of recombinant *Escherichia coli* to spatial dissolved oxygen tension gradients simulated in a scale-down system. *Biotechnol Bioeng*. **93**(2):372–85 (2006).

13. Papagianni M. Methodologies for scale-down of microbial bioprocesses. *J Microb Biochem Technol*. **05**(01):1–7 (2011).

14. Papagianni M, Mattey M, Kristiansen B. Design of a tubular loop bioreactor for scale-up and scale-down of fermentation processes. *Biotechnol Prog*.**19**(5):1498–504 (2003).

15. George S, Larsson G, Enfors S-O. A scale-down two-compartment reactor with controlled substrate oscillations: Metabolic response of *Saccharomyces cerevisiae*. *Bioprocess Eng*. **9**(6):249–57 (1993).

16. Bylund F, Guillard F, Enfors S-O, Trägårdh C, Larsson G. Scale down of recombinant protein production: a comparative study of scaling performance. *Bioprocess Eng*. **20**(5): 377-389 (1999).

17. Sweere APJ, Giesselbach J, Barendse R, Krieger R De, Honderd G, Luyben KCAM. Modelling the dynamic behaviour of *Saccharomyces cerevisiae* and its application in control experiments. *Appl Microbiol Biotechnol*. **28**:116–27 (1988).

18. Delvigne F, Destain J, Thonart P. A methodology for the design of scale-down bioreactors by the use of mixing and circulation stochastic models. *Biochem Eng J*. **28**(3):256–68 (2006).

19. Delvigne F, Destain J, Thonart P. Toward a stochastic formulation of microbial growth in relation to bioreactor performances: case study of an *E. coli* fed-batch process. *Biotechnol Prog*.**22**(4):1114–24 (2006).

20. Delvigne F, Lejeune A, Destain J, Thonart P. Stochastic models to study theimpact of mixing on a fed-batch culture of *Saccharomyces cerevisiae*. *Biotechnol Prog*. **22**:259–69 (2006).

21. Neubauer P., Junne S. Scale-down simulators for metabolic analysis of large-scale bioprocesses. *Curr Opin Biotechnol*. **21**(01):114–21 (2010).

22. Fernandes RL, Nierychlo M, Lundin L, Pedersen a E, Puentes Tellez PE, Dutta A, et al. Experimental methods and modeling techniques for description of cell population heterogeneity. *Biotechnol Adv*. **29**(6):575–99 (2011).

23. Carlquist M, Fernandes RL, Helmark S, Heins A-L, Lundin L, Sørensen SJ, et al. Physiological heterogeneities in microbial populations and implications for physical stress tolerance. *Microb Cell Fact*. **11**(94): 1-13 (2012).

24. Verduyn C, Postma E, Scheffers W a, Van Dijken JP. Effect of benzoic acid on metabolic fluxes in yeasts: a continuous-culture study on the regulation of respiration and alcoholic fermentation. *Yeast*. **8**(7):501–17 (1992).

25. Olsson L, Nielsen J. On-line and in situ monitoring of biomass in submerged cultivations. *Trends in Biotechnol*. **15**(12):517–22 (1997).

26. Villadsen J, Nielsen J, Lidén G. Bioreaction Engineering Principles. Boston, MA: Springer US (2011).

27. Vanoni M, Vai M, Popolo L, Alberghina L. Structural heterogeneity in populations of the budding yeast *Saccharomyces cerevisiae*. *J Bacteriol*. **156**(3):1282–91 (1983).

28. Porro D, Vai M, Vanoni M, Alberghina L, Hatzis C. Analysis and modeling of growing budding yeast populations at the single cell level. *Cytometry A*.**75**(2):114–20 (2009).

29. Odman P, Johansen CL, Olsson L, Gernaey K V, Lantz AE. On-line estimation of biomass, glucose and ethanol in *Saccharomyces cerevisiae* cultivations using in-situ multi-wavelength fluorescence and software sensors. *J Biotechno*l. **144**(2):102–12 (2009).

30. Nevoigt E, Stahl U. Osmoregulation and glycerol metabolism in the yeast *Saccharomyces cerevisiae*. *FEMS Microbiol Rev*. **21**(3):231–41 (1997).

31. Postma E, Verduyn C, Scheffers WA, Van Dijken JP. Enzymic analysis of the Crabtree effect in glucose-limited chemostat cultures of *Saccharomyces cerevisiae*. *Appl Environ Microbiol*. **55**(2):468–77 (1989).

32. Van Dijken JP, Bauer J, Brambilla L, Duboc P, Francois J, Gancedo C, et al. An interlaboratory comparison of physiological and genetic properties of four *Saccharomyces cerevisiae* strains. *Enzyme Microb Technol*. **26**(9-10):706–14 (2000).

33. Van Hoek PIM, Van Dijken JP, Pronk JT. Effect of specific growth rate on fermentative capacity of baker's yeast. *Appl Environ Microbiol*. **64**(11):4226–33 (1998).

34. George S, Larsson G, Olsson K, Enfors S-O. Comparison of the baker's yeast process performance in laboratory and production scale. *Bioprocess Eng*. **18**(2):135–42 (1998).

35. Brauer MJ, Huttenhower C, Airoldi EM, Rosenstein R, Matese JC, Gresham D, et al. Coordination of growth rate , cell cycle , stress response , and metabolic activity in yeast. *Mol Biol Cell*. **19**(1):352–67 (2008).

36. Zakrzewska A, van Eikenhorst G, Burggraaff JEC, Vis DJ, Hoefsloot H, Delneri D, et al. Genome-wide analysis of yeast stress survival and tolerance acquisition to analyze the central trade-off between growth rate and cellular robustness. *Mol Biol Cell.* **22**(22):4435–46 (2011).

37. Sunya S, Bideaux C, Molina-Jouve C, Gorret N. Short-term dynamic behavior of *Escherichia coli* in response to successive glucose pulses on glucose-limited chemostat cultures. *J Biotechnol*. **164**(4):531–42 (2013).

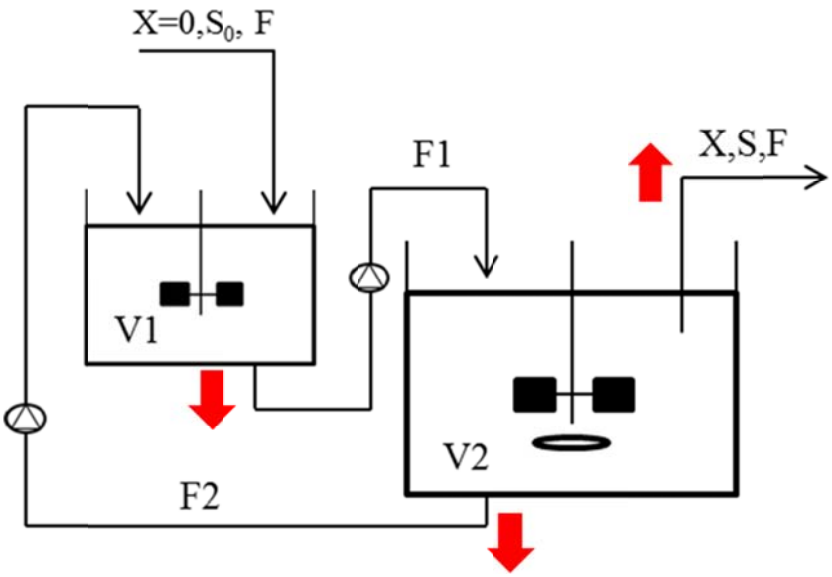

Figure 1 – Ssetup for two-compartment experiments: V_1 represents the 0.5 L reactor with the feed inlet and no oxygen sparging, V_2 represents the remaining reactor volume (3.0 L) with the waste outlet and the oxygen supply. Between the two reactors a recirculation is set up (F_1 and F_2) and samples are taken at three different points, the waste outlet, at the beginning of F_1 as well as at the beginning of F_2. The red arrows mark sampling points.

Table 1 – Overview of factorial design plan: Factorial design with varying glucose feed concentration (50 g/L, 125 g/L and 300 g/L), dilution rate (D = 0.05 h^{-1}, 0.125 h^{-1} and 0.2 h^{-1}) and recirculation flow rate between the two reactors (0.1 L/h, 1.45 L/h and 3 L/h). The asterisk respectively double asterisk marks the experiments that have been performed with the growth reporter strain respectively with both strains.

Run	G_{Feed} [g/L]	D [h^{-1}]	Recirculation flow F_2 [L/h]
A*	300	0.05	0.1
B	300	0.2	0.1
C	300	0.05	3.0
D	300	0.2	3.0
E*	50	0.05	0.1
F**	50	0.2	0.1
G	50	0.05	3.0
H*	50	0.2	3.0
I*	125	0.125	1.45

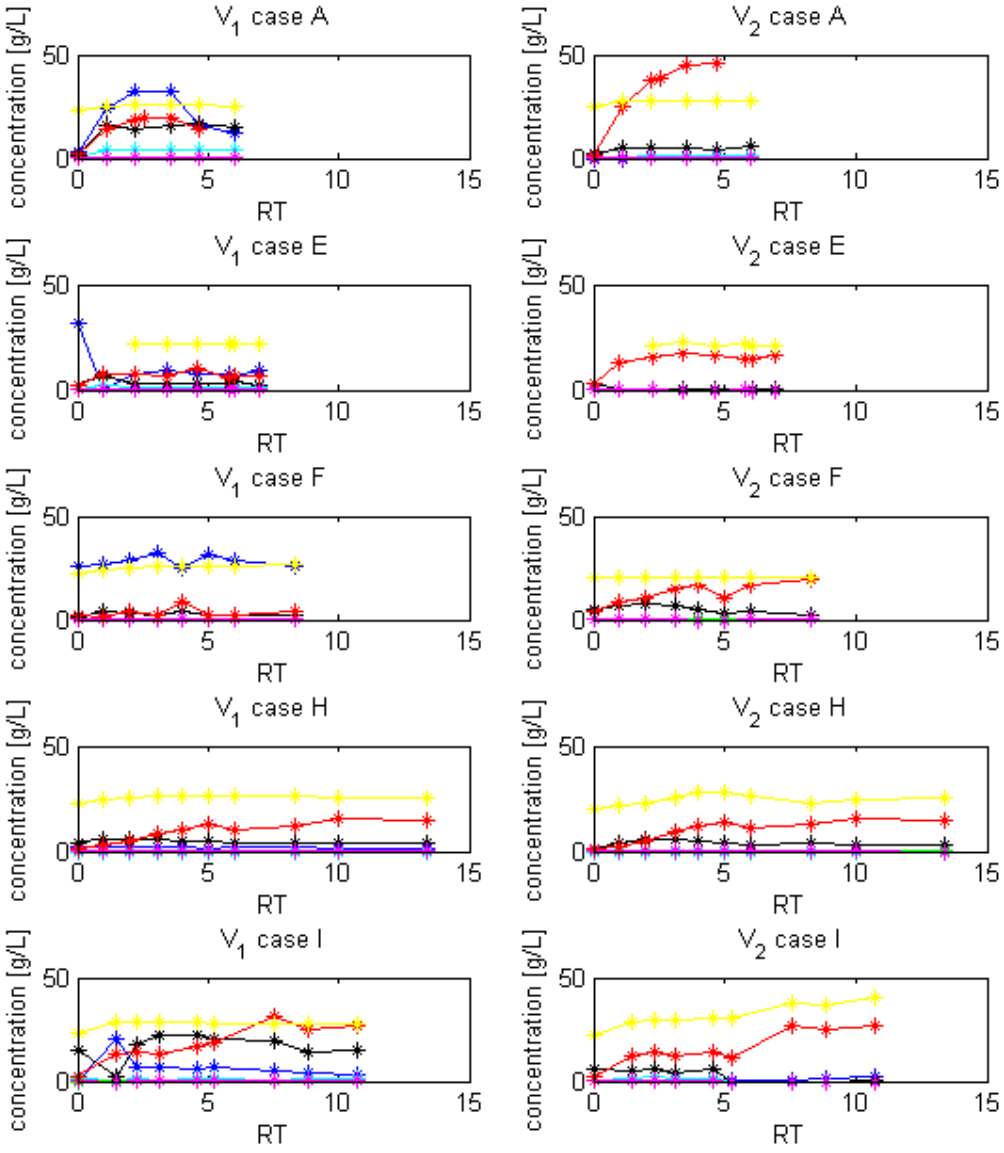

Figure 2 – Variation of glucose, ethanol, glycerol, acetate, pyruvate, biomass and CO_2 for the two-compartment experiments: using the growth reporter strain FE440. Results are shown for the experimentally performed cases (from top to bottom, cases A, E, H, F, I). Blue: glucose; Black: ethanol; Red: biomass; Green: acetate; Yellow: CO_2; Pink: pyruvate; Cyan: glycerol

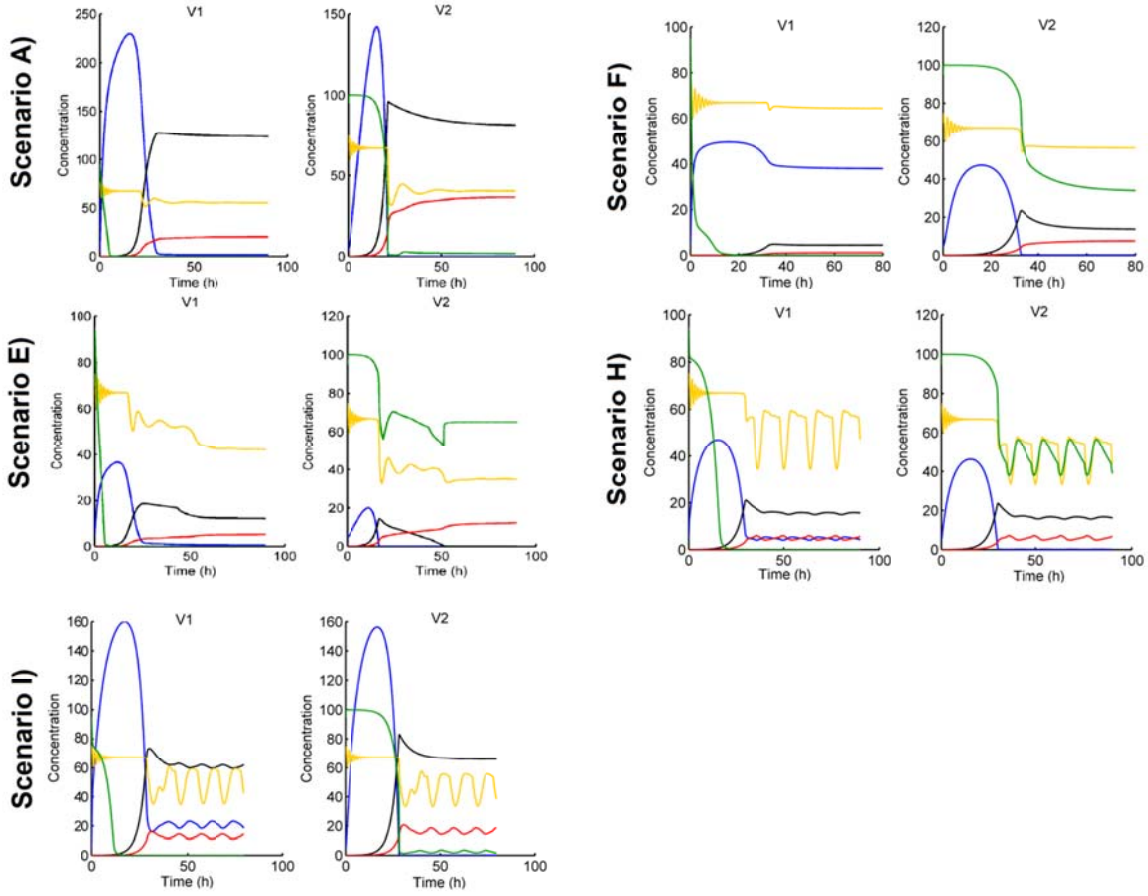

Figure 3 – Variation of glucose, ethanol, glycerol, acetate, pyruvate, biomass and CO_2 for the two-compartment model predictions: results are shown for the experimentally performed cases (A, E, H, F, I). Blue: glucose; Black: ethanol; Red: biomass; Green: dissolved oxygen; Yellow: budding index

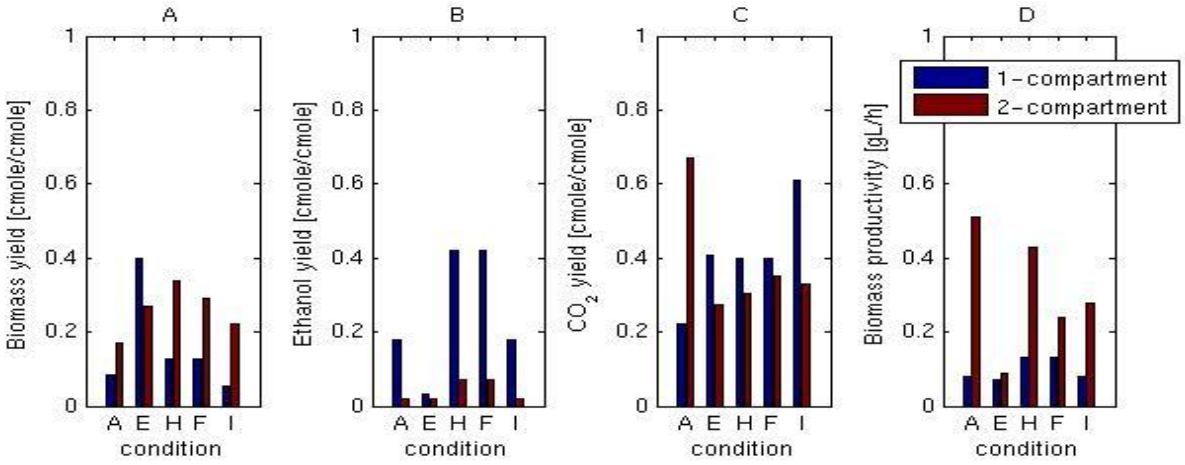

Figure 4 – Biomass, ethanol and CO_2 yields as well as biomass productivity for experiments on glucose: for the one-compartment (blue bars) and the two-compartment (red bars) experiments in steady state.

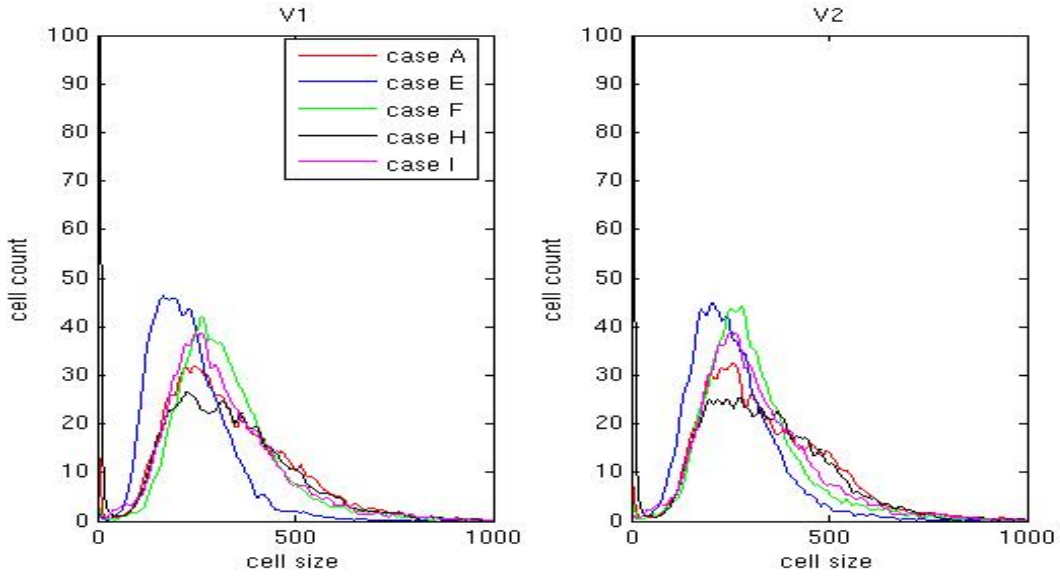

Figure 5 – Variation of the experimental cell size distribution in the two compartments in steady state: using the growth reporter strain FE440. Results are shown for the experimentally performed cases (A, E, H, F, I).

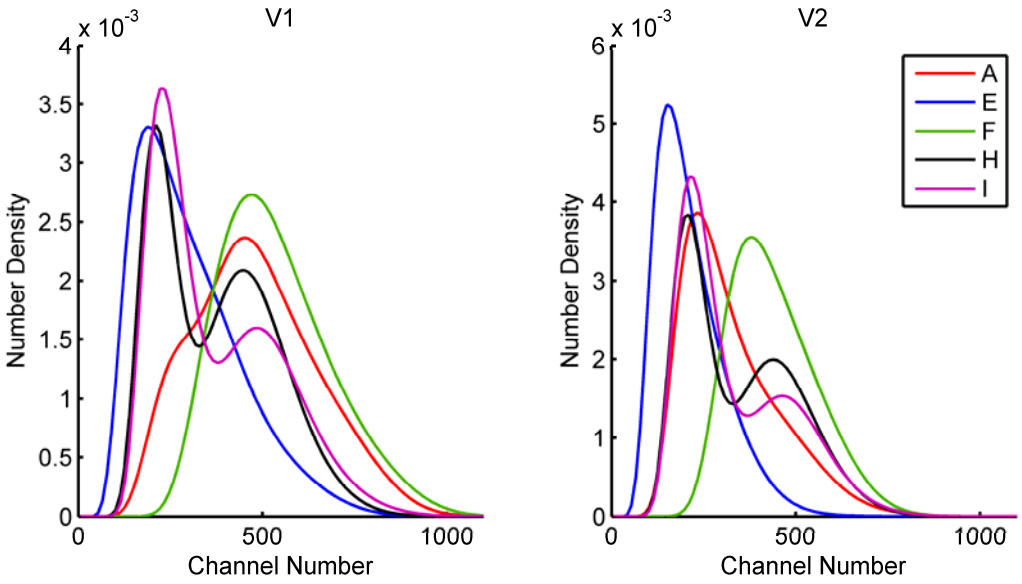

Figure 6 – Variation of the cell size distribution in the two-compartment model: Results are shown for the experimentally performed cases (A, E, H, F, I).

Table 2 – Parameters calculated for cell size in two- and one-compartment chemostats found in experiments and predicted by the model: mean fluorescence and coefficient of variance (CV) calculated for cell size. Values for the two compartments are presented for each compartment separately (V_1 and V_2) and experimental values, including standard deviation, are given as an average for data collected during three subsequent residence times in steady state.

Parameter		**A**	**E**	**F**	**H**	**I**
Model predictions						
Mean	$\mathbf{V_1}$	479.03	300.40	535.76	372	373.62
	$\mathbf{V_2}$	324.10	213.34	439.29	347	334.61
CV	$\mathbf{V_1}$	1.06	1.11	1.03	1.09	1.09
	$\mathbf{V_2}$	1.08	1.10	1.03	1.09	1.09
Experimental results						
Mean	$\mathbf{V_1}$	342.12±5.1	230.02±34.51	330.12±0.71	333.79±41.62	343.47±3.6
	$\mathbf{V_2}$	345.79±4.6	233.56±4.15	307.13±3.6	306.53±14.48	348.37±41.11
CV	$\mathbf{V_1}$	0.66	0.46	0.58	0.80	0.58
	$\mathbf{V_2}$	0.66	0.43	0.55	0.77	0.62

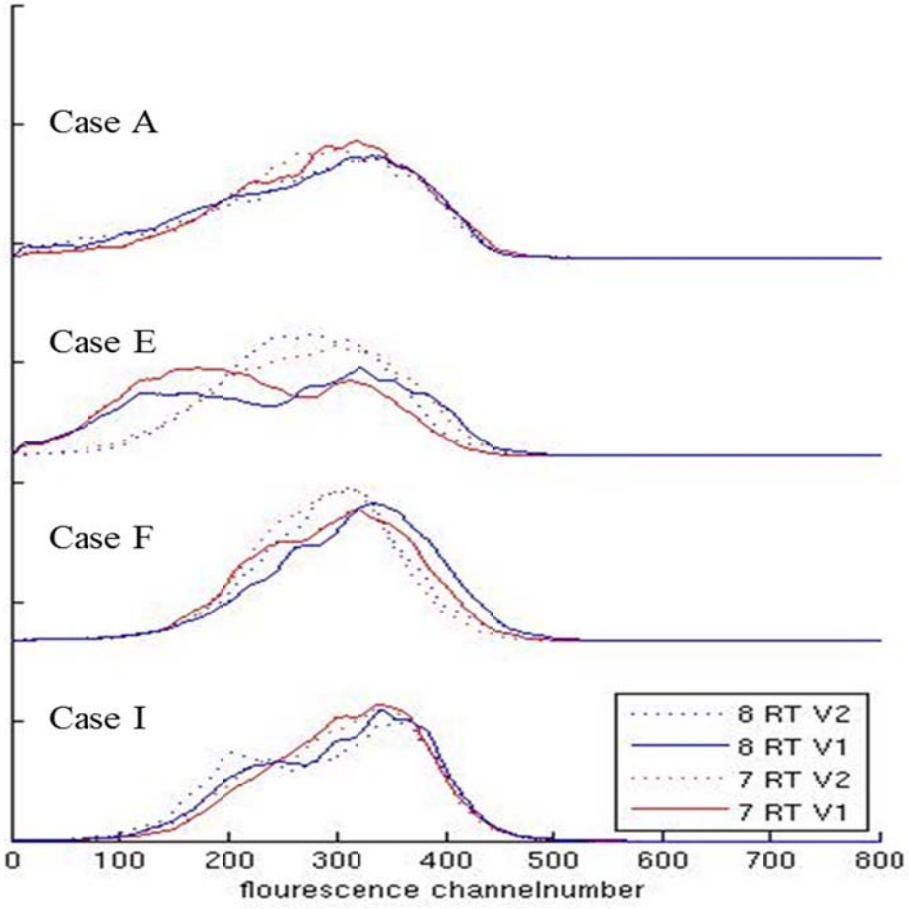

Figure 7 – histogram plots for experimental GFP fluorescence/membrane robustness data in steady state: after applying freeze-thaw stress using the growth reporter strain FE440. Plots are shown as a comparison between the different compartments (V_1 and V_2) of the two-compartment setup for two subsequent residence times in steady state.

Table 3 – Parameters calculated for objective description of membrane robustness in two- and one-compartment experiments: mean fluorescence and coefficient of variance (CV) calculated for GFP fluorescence in the two-compartment setup and the one-compartment setup. Values for the two compartments are presented for each compartment separately (V_1 and V_2) and all values are given including standard deviation as an average for three subsequent residence times in steady state.

Parameter		**A**	**E**	**F**	**I**
Mean	**V_1**	268.83± 9.89	222.39± 20.58	308.23±10.34	310.34±10.01
GFP	**V_2**	259.57±12.03	280.71± 20.74	295.43± 9.07	298.91±7.49
	Chemostat	342.91± 0.26	288.95 +/-35.57	361.32±27.98	396.64± 3.84
CV	**V_1**	0.41	0.52	0.24	0.24
	V_2	0.46	0.56	0.23	0.26
	Chemostat	0.33	0.42	0.31	0.21

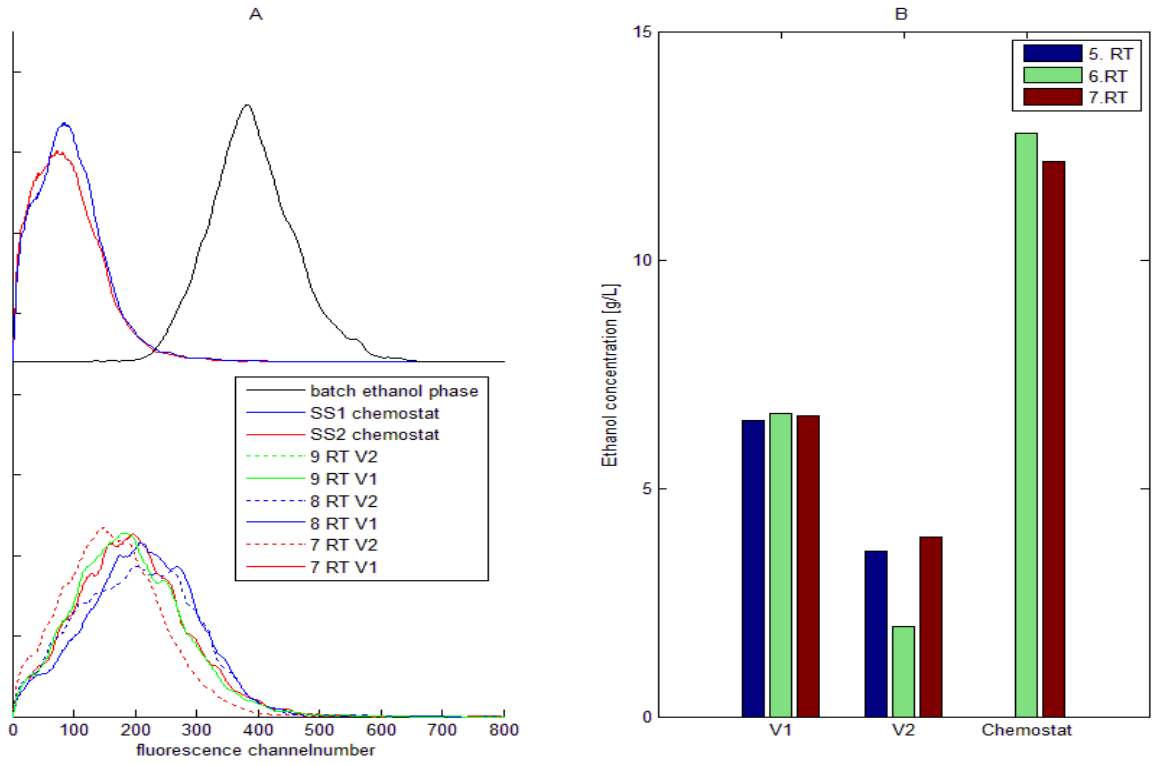

Figure 8 – BFP fluorescence/ ethanol respectively glucose consumption in steady state: using the ethanol reporter strain Sc-PCK1-B grown at D = 0.2 h^{-1} with 50 g/L feed concentration and low recirculation (case F). Plots are shown as a comparison between the different compartments (V_1 and V_2) of the two-compartment setup and the one-compartment setup for three subsequent residence times in steady state in a histogram plot (A). Furthermore, as a positive control a distribution of the batch phase during ethanol growth is included (black).In addition ethanol concentration values are shown for the samples shown as distribution (B).

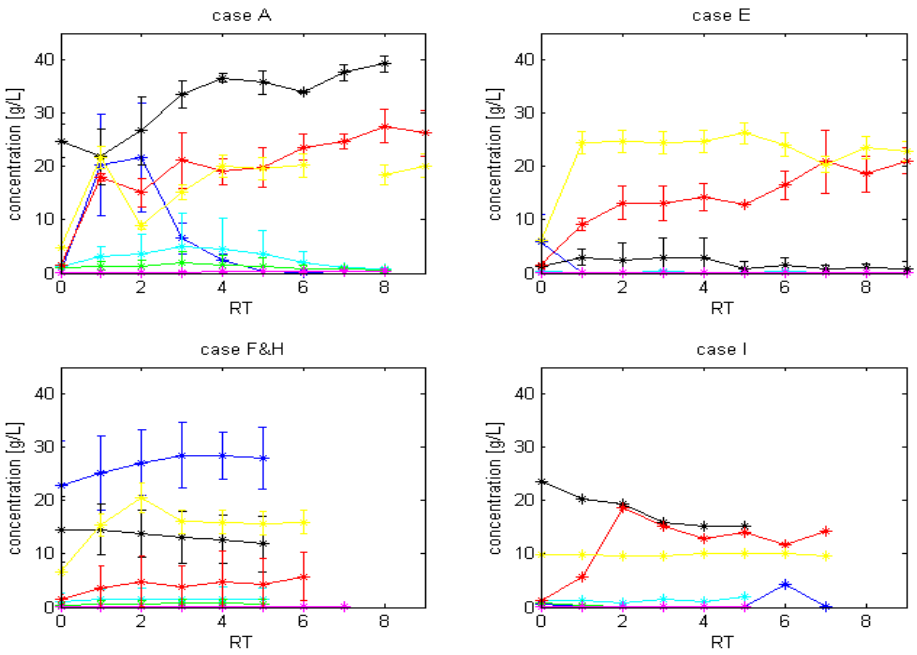

Figure 9 – Variation of glucose, ethanol, glycerol, acetate, pyruvate, biomass and CO_2 for one-compartment experiments: using the growth reporter strain FE440. Results are shown for the experimentally performed cases (A, E, H, F, I). Blue: glucose; Black: ethanol; Red: biomass; Green: acetate; Yellow: CO_2; Pink: pyruvate; Cyan: glycerol

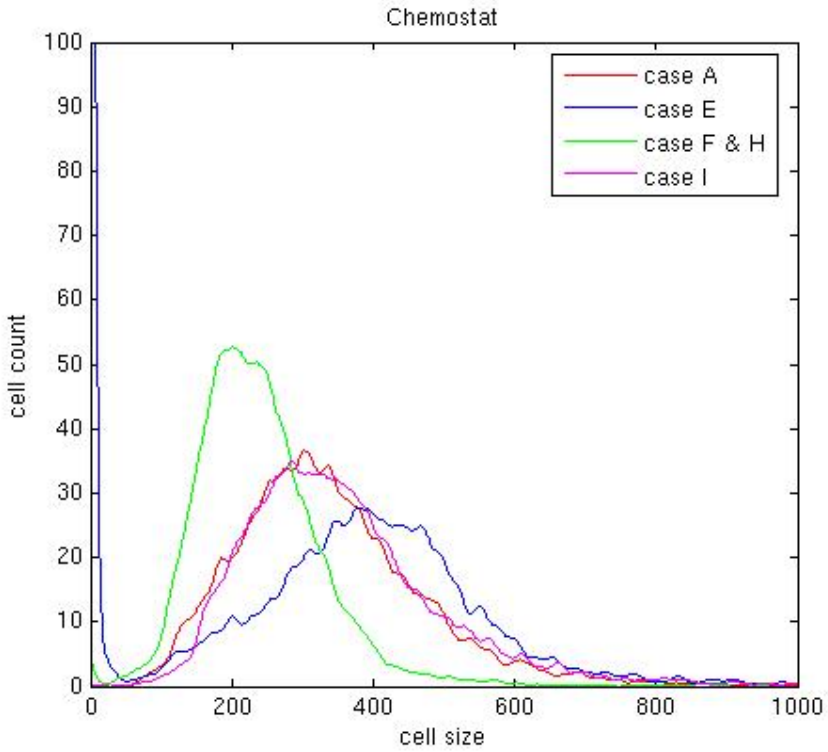

Figure 10 – Variation of the experimental cell size distribution in steady state for one-compartment experiments: using the growth reporter strain FE440. Results are shown for the experimentally performed cases (A, E, H, F, I).

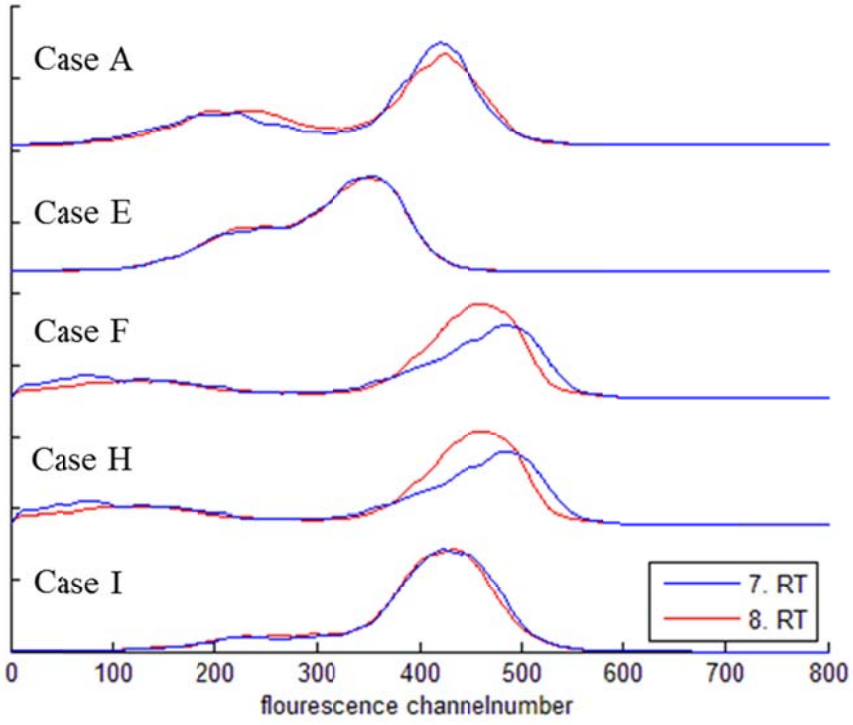

Figure 11 – Histogram plots for GFP fluorescence/membrane robustness data in steady state for one-compartment experiments: after applying freeze-thaw stress using the growth reporter strain FE440. Plots are shown as a comparison between the different cases (A, E, F, H and I) for two subsequent residence times in steady state.

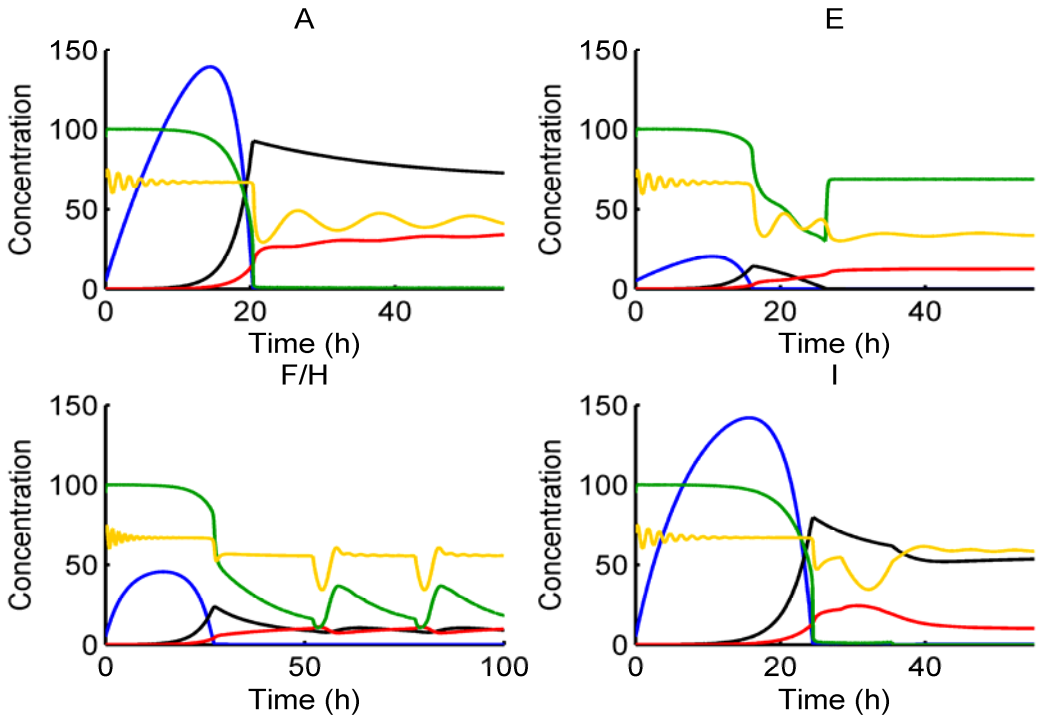

Figure 12 – Variation of glucose, ethanol, glycerol, acetate, pyruvate, biomass and CO_2 for one-compartment model: results are shown for the experimentally performed cases (A, E, H, F, I). Blue: glucose; Black: ethanol; Red: biomass; Green: dissolved oxygen; Yellow: budding index.

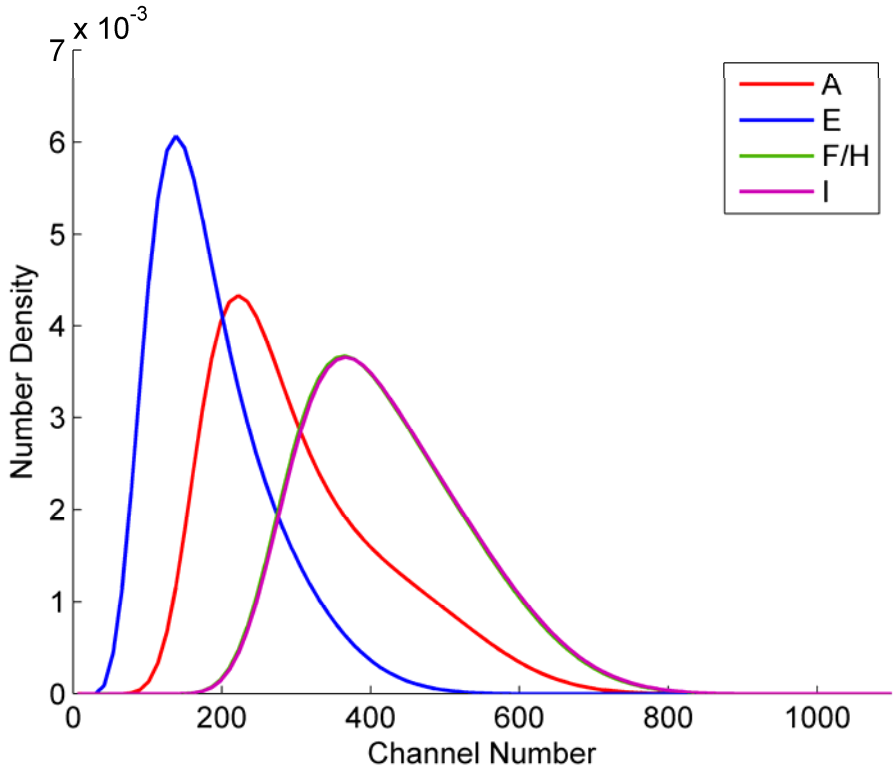

Figure 13 – Variation of cell size distribution for one-compartment model: results are shown for the modeled cases (A, E, H, F, I)